

## Beam Scanning of Silicon Lens Antennas Using Integrated Piezomotors at Submillimeter Wavelengths

Alonso Del Pino, Maria; Jung-Kubiak, Cecile; Reck, Theodore; Llombart , Nuria; Chattopadhyay, Goutam

**DOI**

[10.1109/TTHZ.2018.2881930](https://doi.org/10.1109/TTHZ.2018.2881930)

**Publication date**

2019

**Document Version**

Accepted author manuscript

**Published in**

IEEE Transactions on Terahertz Science and Technology

**Citation (APA)**

Alonso Del Pino, M., Jung-Kubiak, C., Reck, T., Llombart , N., & Chattopadhyay, G. (2019). Beam Scanning of Silicon Lens Antennas Using Integrated Piezomotors at Submillimeter Wavelengths. *IEEE Transactions on Terahertz Science and Technology*, 9(1), 47-54. Article 8537949.  
<https://doi.org/10.1109/TTHZ.2018.2881930>

**Important note**

To cite this publication, please use the final published version (if applicable).  
Please check the document version above.

**Copyright**

Other than for strictly personal use, it is not permitted to download, forward or distribute the text or part of it, without the consent of the author(s) and/or copyright holder(s), unless the work is under an open content license such as Creative Commons.

**Takedown policy**

Please contact us and provide details if you believe this document breaches copyrights.  
We will remove access to the work immediately and investigate your claim.

# Beam Scanning of Silicon Lens Antennas Using Integrated Piezo-Motors at Submillimeter Wavelengths

Maria Alonso-delPino, *Member, IEEE*, Cecile Jung-Kubiak, *Senior Member, IEEE*, Theodore Reck, *Senior Member, IEEE*, Nuria Llombart, *Senior Member, IEEE*, and Goutam Chattopadhyay, *Fellow, IEEE*

**Abstract**—This paper presents a lens antenna that scans the beam using an integrated piezo-motor at submillimeter wave frequencies. The lens antenna is based on the concept presented in [1], a leaky wave waveguide feed in order to achieve wide angle scanning and seamless integration with the receiver. The lens is translated from the origin of the waveguide producing the scanning of the beam over a 50 deg Field of View (FoV) (or about 6.25 beamwidths) with a maximum scanning loss of 1 dB. The lens movement is achieved with a piezoelectric motor that is integrated within the antenna and receiver block. A prototype was built and measured at 550 GHz achieving scanning beam angles close to 20 degrees with only 0.6 dB of loss. The scanning of the 50 deg FoV, which corresponds to a lens displacement of approximately 2 mm, takes about 0.9 s achieving a scanning rate of 0.75 Hz of the FoV. The accuracy in continuous mode of the piezo actuator has been measured to be less than  $28\mu\text{m}$  in the worse of cases for displacements of 2 mm, which corresponds to a beam steering of 0.76 deg, much smaller than the antenna half power beamwidth of 8 deg.

**Index Terms**—Beam-scanning, piezo-motor, silicon lens, leaky-wave waveguide feed, submillimeter-wave.

## I. INTRODUCTION

SUBMILLIMETER-WAVE heterodyne instruments enables high resolution observations of many chemical species that are of importance for the understanding of planetary atmospheres [2], [3], comet composition [4], [5] or interstellar medium evolution [6]. The imaging of the FoV is usually performed by the combination of the spacecraft movement and the optical system scanning [5]. When a faster imaging of the field of view is required, focal plane array systems reduce the imaging speed by a factor equal to the number of elements on the array [7]. However, this approach increases the power, mass, and volume of the instrument, which for some space missions, is not viable.

The state of the art of submillimeter-wave instrumentation that performs beam-scanning relies on electromagnetic motors, i.e. brushed or brushless DC motors and stepper motors, which are high weight and power, and some of them can even introduce excessive heat and vibrations into the rest of

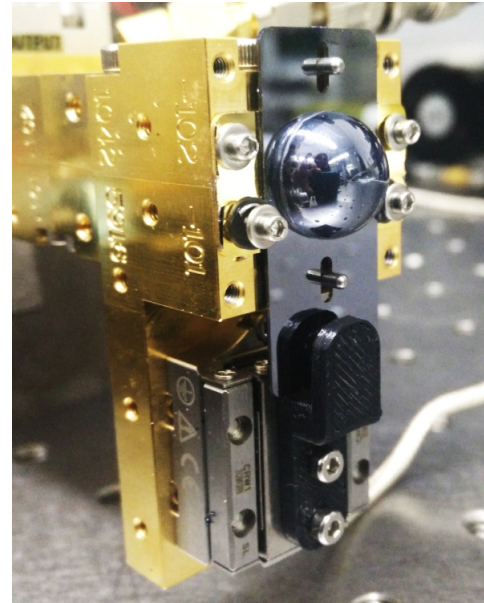


Fig. 1: Photograph of the prototype at 550 GHz of the silicon lens fed by a leaky-wave waveguide feed with an integrated piezo-electric motor. The hemispherical silicon lens has a radius of 6 mm.

the system components. For example, the near-field imaging radar in [8] uses a high power brushless motor to move a flat mirror, and weights around 4 kg. Other examples such as the Submillimeter-Wave Instrument (SWI) in JUICE or TEMPEST-D use a stepper motor to rotate the primary reflector and, the SWI, another one that rotates the whole instrument [9].

Piezo-electric actuators are non-electromagnetic motors, and use a piezo material (a crystal or ceramic) that deforms under an electrical field to convert this electrical energy into a mechanical deformation. Piezo-electric motors convert this small deformation into a large motion through friction. It has a behavior that compares to an electrical capacitor, thus, consumes very low power and no heat is generated. One of their drawbacks, initially, was their shorter lifetime and reliability, but lately this has been improved by using fully qualified and robust manufacturing processes. With continuous advances in piezoelectric technology, one can find a wide variety of actuators that range different performances and are

Manuscript received November X, 201X; revised January 03, 201X.

Copyright 2018 California Institute of Technology. U.S. Government sponsorship acknowledged.

M. Alonso-delPino, C. Jung-Kubiak, T. Reck and G. Chattopadhyay are with the Submillimeter-Wave Advance Technology group at the Jet Propulsion Laboratory, California Institute of Technology, Pasadena, CA. 91109 USA (e-mail: maria.alonso@jpl.nasa.com). N. Llombart is with the Terahertz Sensing group at the Technical University of Delft, The Netherlands.

suitable for a wide range of applications [10]. They have been used in the drilling system of the Mars Rover Curiosity or in the dust analysis instrument Midas from Rosetta. In this work we propose the integration of this piezo-electric technology in our receivers in order to enable a low power, mass and volume beam-scanning mechanism.

The key requirement for a submillimeter- receiver is to have a highly compact low loss, waveguide based, packaged system. Silicon micromachining based on DRIE (Deep Reactive Ion Etching) is an enabling technology that allows the fabrication of 3D structures on silicon wafers with high accuracy [11]. This technology has been used for the fabrication of heterodyne submillimeter wave system front ends as in [12], [13] and be integrated with the more traditional split metal block technology [14]. For these front ends, a silicon micro-lens fed by a leaky-wave cavity [1], [15], [16] proved to be the most viable solution in terms of performance, fabrication, and integration either in silicon or metal machining up to 1.9 THz [14]. Furthermore, compared to traditional horn antennas, this antenna architecture enables scanning capabilities. Moreover, the air-gap that realizes the leaky wave cavity facilitates the relative translation between the lens and waveguide feed. This has enabled us to combine piezoelectric technology with our silicon micro-machining capabilities to integrate a very small motor based on piezo movement in our silicon wafer stack, see Fig. 1. The off-axis performance of integrated silicon antennas coupled to planar antennas was investigated in [17], [18]. There has been other approaches to integrate mechanical movement on lens antennas at millimeter-wavelengths [19]. However, to the best of our knowledge, there has not been a demonstration of integrated piezo-electric motors with lens antennas at submillimeter wavelengths.

The aim of this paper is to present the scanning capabilities and performance of a silicon lens fed by a leaky wave feed at 550 GHz and its integration and testing with a piezo-electric motor. Since piezo-electric motors are light weight and low power, the proposed antenna could enable future space instruments replacing the bulky opto-mechanical systems. Section II describes the architecture and scanning properties of the micro-lens antenna. Section III describes its integration with a piezoelectric actuator. Section IV shows the measurement setup and results of a prototype built at 550 GHz as well as the performance of the piezo electric actuator. The conclusions are drawn at the end.

## II. SCANNING PROPERTIES OF THE SILICON LENS ANTENNA

The lens antenna geometry consists of a leaky waveguide feed that provides a very directive feed that illuminates only the upper part of an extended hemispherical lens [1]. The feed is composed of a square waveguide, an iris on a ground plane and an air gap between the iris and the silicon lens, shown in Fig. 2. The waveguide couples the radiation from the device layer containing the front-end receiver circuit to the iris, air gap and lens. The semi-hemispherical extended silicon lens sits on top of the air cavity.

In previous works, the proposed lens antenna was very shallow because it was truncated at a certain angle [16] to

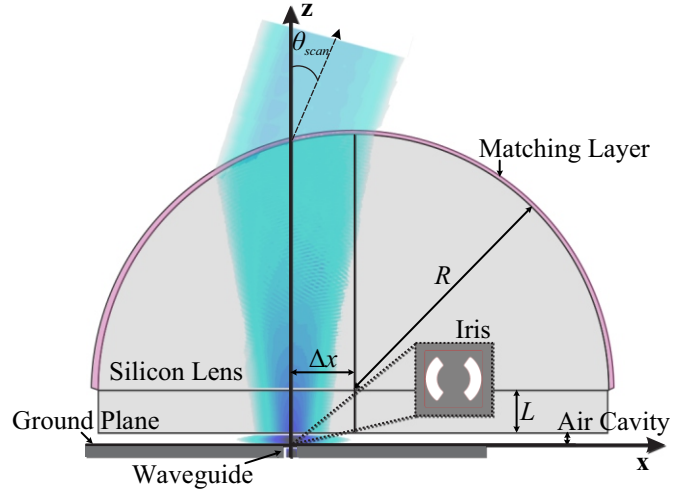


Fig. 2: Illustration of the scanning silicon lens-antenna geometry. The lens is translated from the waveguide nominal position producing the scanning of the beam.

achieve closed packed focal plane arrays. Instead, in this effort, we propose the use of a full hemispherical lens in order to avoid any spill-over losses while scanning and therefore enlarging the scanning range. We present here the scanning performance of a silicon lens with radius of  $R = 11\lambda = 6\text{mm}$ . Such antenna will couple to an external quasi-optical system with an f-number around 3. We have used the combination of a full wave simulation, to obtain the filed patterns radiated by the leaky-wave fed in an infinite medium, and Physical Optics, to evaluate the radiation of the lens antenna in free space, as explained in [16].

Fig. 3 shows parametric studies of the directivity (a) and Gaussicity (b) versus the extension height  $L$  and the lens displacement  $\Delta x/R$  from the center of the leaky wave feed. The contour plots in the figure describe a strong variation due to the high index of refraction of the lens. The maximum of the directivity is found at a very low extension length, around  $L/R = 0.04$ , compared to the well-known guidelines of the double slot antenna [18],  $L/R \approx 0.39$ , since the leaky wave has a phase center behind the ground plane. The directivity variation while scanning at these optimum extension lengths is much lower in the case of the leaky wave feed (less than 1dB drop until scanning of around 23.5 degrees as shown in Fig. 3a). Moreover the reflection losses at this extension while scanning are also much lower than in the double slot case (see Fig. 3a) thanks to the illumination of the top part of the lens only (see Fig. 2). Indeed, the leaky wave feed has a taper illumination angle of -10/-14 dB at around 15 degrees compared to the 50-60 degrees in case of the double slot.

Generally, for submillimeter-wave heterodyne systems, this lens antenna is coupled to a quasi-optical system, and hence, the Gaussicity is an important parameter for defining the feed scanning performance. The Gaussicity is calculated using [20] optimizing the Gaussian beam parameters (waist and phase center) at zero displacement for each extension length. The Gaussicity for non-zero displacements is evaluated with

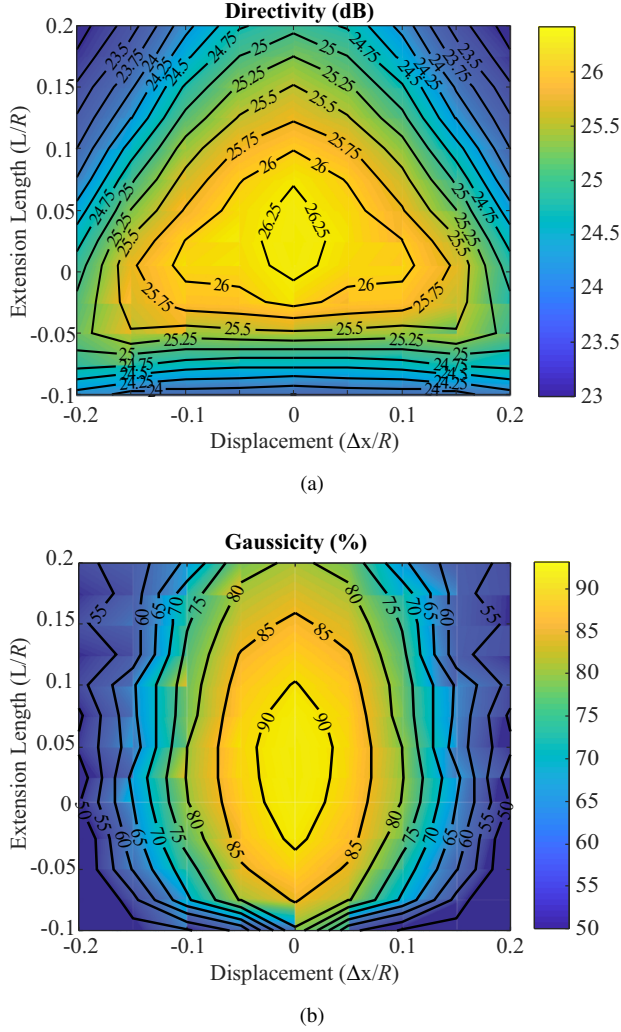


Fig. 3: Directivity (a) and Gaussiaicity (b) as a function of the lens extension length and the lens displacement from the center of the feed for a lens radius of  $R = 11\lambda = 6\text{mm}$  hemispherical lens at 550 GHz.

these same Gaussian beam characteristics and plotted in Fig. 3b versus the extension length and lateral displacement. As opposed to [18], the maximum Gaussiaicity for this system is achieved at the extension height that leads to the highest directivity.

Therefore, using an extension height  $L = 0.04R$  will lead to a high coupling efficiency to an external quasi-optical system for a wide angle scanning. This lens antenna has a maximum scanning directivity loss of -1 dB, a Gaussiaicity better than 65% and reflections losses lower than 0.1 dB over a  $\pm 23.5$  degrees scanning range. The angular half-power beamwidth is 8 deg, which leads to about 6.25 beams in the FoV. Based on these dimensions, we built a prototype antenna operating at 550 GHz. To achieve the mentioned scanning range, a translation of the lens of  $\pm 0.96\text{mm}$  with a resolution better than 0.32 mm is required.

The proposed lens prototype with an ideal quarter wave-length matching layer ( $\epsilon_{rm} = \sqrt{11.9}$ ) has also been simulated using a full wave solver in order to include the effects of

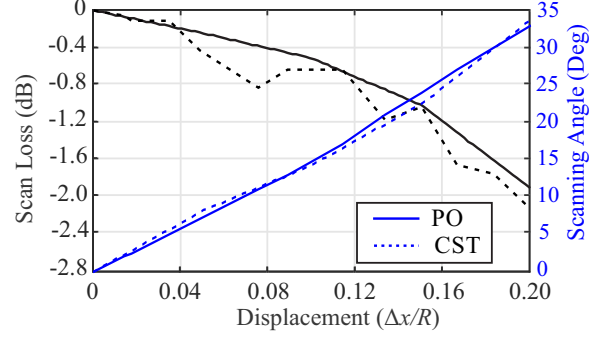


Fig. 4: (Left Axis) Scan loss and (Right Axis) scanning angle as a function of the lens displacement of the lens-antenna for  $L = 0.04R$ .

the multiple reflections [21]. The obtained scan loss and scan angle are shown in Fig. 4. The agreement is very good with the PO simulations, even though there are some oscillations associated to the multiple reflections. The values of Gaussiaicity are also very similar.

### III. INTEGRATION OF THE PIEZO-ELECTRIC MOTOR

The key enabling technology to perform a fast and accurate scanning of the feed is the advancement of piezo-electric actuator motors. We built a lens-antenna prototype with a piezo electric motor at 550 GHz. The piezoelectric motor is a commercial miniature linear stage from PI Motion Positioning [10]. The linear movement is based on a piezoelectric inertia drive which achieves, according to the manufacturer specifications, a pull/push force of 1 N, speeds of 10 mm/s and travel ranges of 12 mm with a 1 nm resolution. With its very small size of around  $2\text{ cm} \times 2\text{ cm} \times 1\text{ cm}$  it can be integrated within the same metal block of the receiver.

The overall assembly consists of a metal block, where the receiver or the Local Oscillator will be integrated, with the piezo actuator and silicon wafers laying on top containing the antenna and/or further receiver circuitry. To show the operability and performance of the antenna architecture, the prototype built is based on a split block that contains the piezo electric actuator with the antenna system which can be plugged into one of our existing sources at 550 GHz for measurement (see Fig. 1 and 5). There is a gold plated silicon wafer that contains the iris membrane with the double slot and it is placed on top of the metal block. This wafer is aligned to the metal block using silicon pins as in [14] and is fixed to the metal block using screws with washers. On top of this, another silicon wafer is used to define the air cavity and the extension length of the lens. All the wafers are processed using DRIE based silicon machining as in [14].

The silicon lens is a 12 mm radius semi-hemisphere (commercially available from Tydex) and is coated with a 550 GHz anti-reflection coating layer of Parylene. A series of concentric circles were etched to the silicon wafer to define the exact position of the lens taking into account its fabrication tolerances of the diameter, which was  $\pm 0.1\text{mm}$ .



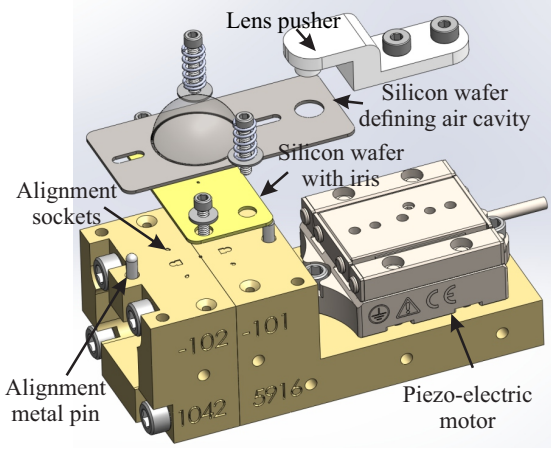


Fig. 5: Sketch of the proposed assembly of the prototype at 550 GHz of the silicon lens or  $R = 6\text{mm}$  fed by a leaky-wave waveguide feed with an integrated piezo-electric motor.

The two silicon wafers, the one containing the iris and the one holding the lens are optically polished, which, by having a low coefficient of friction, provide a clean and smooth translation surface. Moreover, the airgap between the feed and silicon lens favors the translation movement of the lens without damaging the membrane. Two metal pins define the alignment of the lens with the feed in the axis perpendicular to the movement, and define the movement direction of the lens. The feed is screwed to the actuator and the lens can be pushed back and forth for scanning purposes. The lens is placed flat against the feed wafer using screws with a spring in order to regulate the pressure applied in the interface.

#### IV. MEASUREMENT SETUP AND RESULTS

Two set of measurements were made to evaluate the performance of the antenna architecture and piezo-electric motor capabilities. To perform the antenna measurements, we built a far-field measurement set up at WR-1.5. We assembled a JPL developed 550 GHz transmitter chain based on Schottky multiplier devices, transmitting an overall power around 2 - 2.5 mW between the 520-550 GHz band (see inset of Fig. 6). The antenna was connected to this source and placed on two rotational stages that moved the assembly in elevation and azimuth (see Fig. 6). A WR-1.5 frequency extender was used as a receiver on the other end. A standard horn and wire grid was used to measure both polarizations. A PNA-X controlled by a computer was used as a synthesizer for both sources and to process the received signal. More than 60 dB of dynamic range was achieved using this configuration, which was sufficient to measure co and cross polarizations.

##### A. Antenna Measurements

The reflection coefficient of the antenna was measured with the PNA-X and calibrated WR 1.5 frequency extender to first verify the assembly. Fig. 7 shows the reflection coefficient of the antenna as a function of the frequency and plotted against

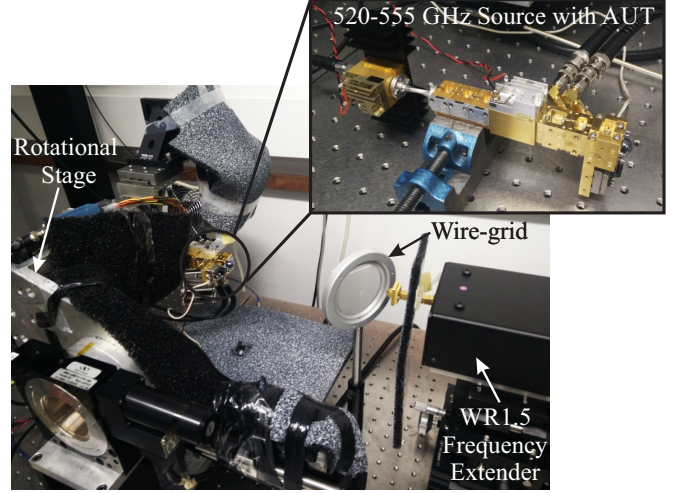


Fig. 6: Photograph of the antenna far-field measurement setup with a 520-555 GHz source with our antenna under test (AUT) mounted on two rotational stages. A WR1.5 frequency extender is used as a receiver.

the simulations. Since the reference plane for calibration for the transceiver was at the beginning of the metal block fixture, the losses in the block lower down the overall reflection values as seen in simulation comparison (dash line). The simulations have been performed using the Time Domain Full wave simulator CST [22] setting the waveguide metal conductivity to  $\sigma = 5e6\text{S/m}$ , that was measured in previous prototypes. The losses estimated in the waveguide transition are 2.8 dB at 550 GHz. The overall shape and performance agrees well with simulations. By moving the lens back and forth with the piezo electric motor while verifying that the reflection coefficient did not have significant changes, we calibrated the compression of the spring with screws that tightened the lens to the feed. Overall, the reflection coefficient is below -13 dB on a bandwidth of more than 15% which should be suitable for most of our heterodyne instruments. The measurement shows consistency across the back and forth movement of the lens by the piezo actuator motor.

The measured co- and cross-polar radiation pattern when the lens was positioned in the center is shown in Fig. 8. The receiver and wire-grid were rotated by 90 degrees to measure the cross-polarized field. The measurements show good agreement with the full-wave simulation results. The cross-pol level is below 20 dB from the co-polarized field which is reasonable for majority of our applications.

The directivity was measured over the 520 GHz to 575 GHz band and is shown in Fig. 9. Above and below the band there was not enough transmitted power from the source to have a sufficient dynamic range to measure the antenna. The gain was measured on the 520 GHz to 550 GHz band; above 550 GHz the transmitted power was not measured accurately and the power calibration was not truthful. The disagreements between measurements and simulations are within the tolerances of the measurement setup and fabrication/assembly, moreover the use of a Parylene matching layer ( $\epsilon_r \approx 2.5$ )

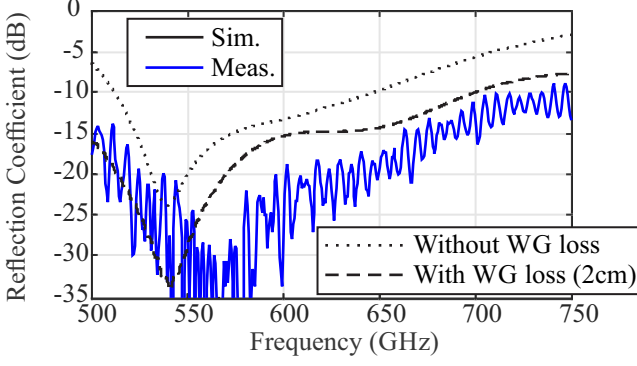


Fig. 7: Reflection coefficient as a function of the frequency for the full WR1.5 band. The measured reflection coefficient contains 2 cm of waveguide losses (Ohmic loss) from the metal block fixture where the antenna is assembled.

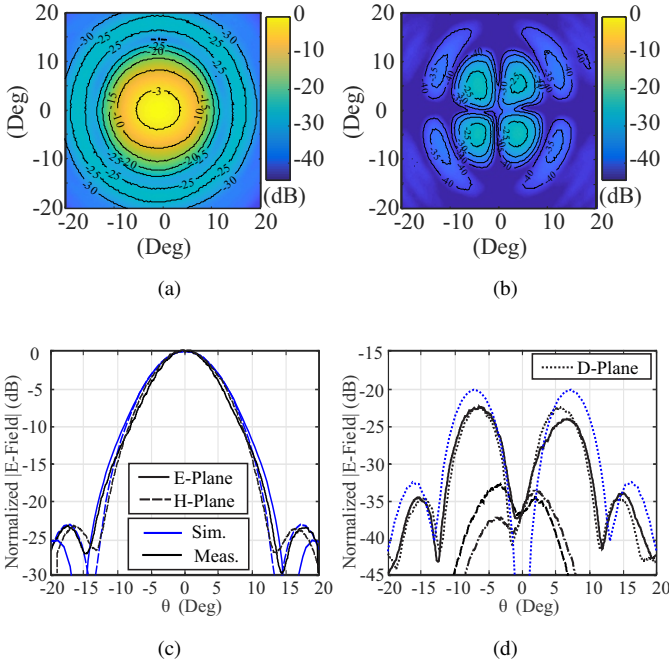


Fig. 8: Measured (black) and simulated (blue) co- and cross-polarized radiation patterns at 550 GHz.

instead of an ideal one ( $\epsilon_r \approx 3.45$ ) increases the impact of the multiple reflections in the lens directivity and gain.

### B. Scanning Performance

The proposed scanning antenna performs a continuous scanning, but, for simplicity, the scanning performance of the proposed lens antenna was measured at various discrete lens positions at the central frequency of 550 GHz. The measured patterns against the full wave simulated patterns are shown in Fig. 10. The main lobe of the radiation patterns has a good agreement with the simulations. However, when the lens is

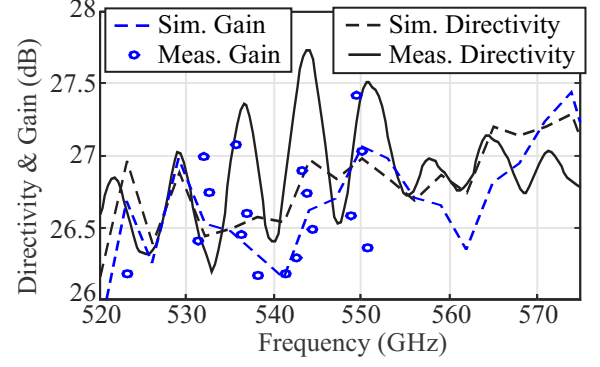


Fig. 9: Measured and simulated directivity and gain as a function of the frequency.

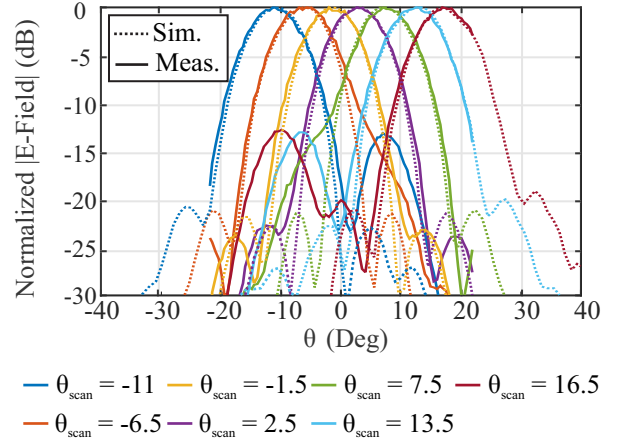


Fig. 10: Measured (solid line) and simulated (dashed line) radiation patterns at different scanned positions at 550 GHz.

displaced from the center position a secondary lobe appears at around -13dB, not present in the simulations.

The secondary lobe appearing on the measurements is due to the reflections of the lens. The simulations in Fig. 11 show the results for an ideal antireflective coating for silicon. Even though Parylene is close to the desired permittivity ( $\epsilon_{rm} \approx 2.1$ ), the difference can be clearly perceived especially when the lens is off-axis from the feed. Fig. 11 illustrates this effect, where the radiation patterns are plotted for a perfect matching layer, Parylene matching layer (reflection loss of 0.3 dB) and no matching layer (reflection loss of 1.42 dB). Overall, Parylene reduces the sidelobes to -13 dB, from -7 dB when no matching layer is used. For applications requiring a lower side-lobe level, one can mitigate further the reflections by patterning subwavelength features on the silicon lens surface creating a perfect anti-reflection coating [23]. Another option is to use other materials based on mixed epoxies (i.e. Stycast as in [24]) that achieve a closer match to silicon. The last option is to use a patterned resistive layer, between the lens and the feed to absorb the second reflection that comes back from the lens [25], in order to avoid the interference of this side-lobe with the observation.

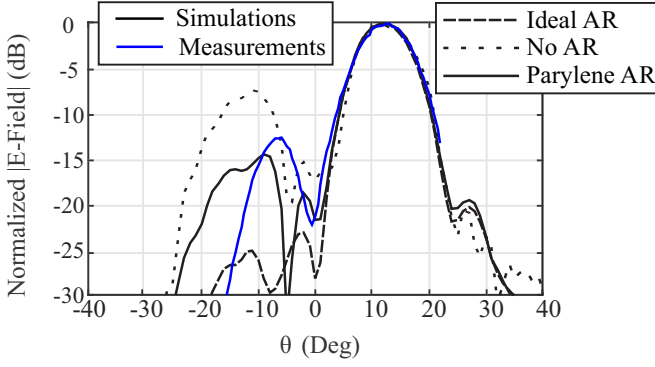


Fig. 11: Measured (blue line) and simulated (black line) radiation pattern at  $\Delta x = 500\mu m = 0.83\lambda$  when using a perfect matching layer, Parylene, and no matching layer.

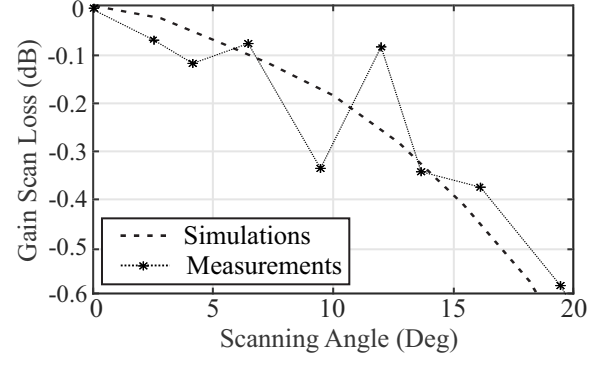
The overall scanning loss as a function of scanning angle is summarized in Fig. 12a. This loss as a function of the scanning angle is calculated by measuring the peak power value at each lens position and compared to the gain drop evaluated via the PO simulations. The agreement between simulations and measurements is good, note the discrepancies are due to the power fluctuations, limitations of the measurement setup and increases of reflection loss due to the Parylene layer.

The scanning angle is plotted against the displacement in Fig. 12b. Overall, the experimental results follow the predictions obtained from the simulations, which demonstrates the operability and performance of the antenna architecture proposed.

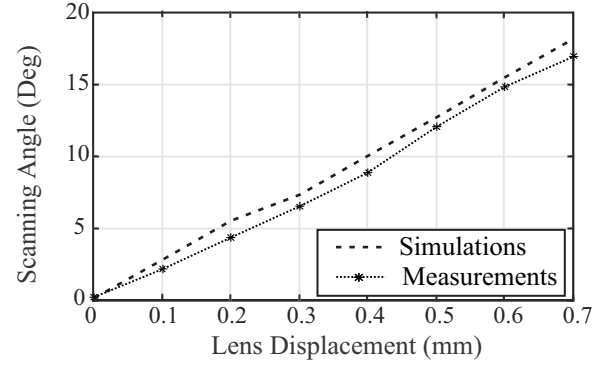
### C. Piezo-electric Motor Performance

We performed a series of tests to ascertain the speed and accuracy of the piezo electric actuator motor. The piezo electric motor has an integrated motion sensor that records the position of the scanning for each instant of time. When the stage is used with a discrete motion (stopping at each pointing angle), the accuracy of the position is around 1 nm. However, when the piezo is used in continuous mode, one might expect the accuracy to decrease. We performed an experiment that consisted on continuously moving the stage back and forth for about 20 loops and record its position at each instant of time. The travelling range was 1 mm and set to a maximum speed of 10 mm/s. Fig. 13a shows the recording of the position for each loop on the right axis, and the left axis shows the standard deviation of the position at each instant of time. The maximum deviation of the position measured was 28  $\mu m$ . We observe that the error is concentrated at the center of the displacement of the translation movement and the accuracy for both, push and pull force operations are similar. The achieved deviation is well-below the requirement (320  $\mu m$ ).

From the movement slope depicted in Fig. 13a, we extracted the speed of the piezo electric actuator for travelling ranges ranging from 0.5 mm to 6 mm (see Fig. 13b). The acceleration for the three displacements was measured to be around 11.5 mm/s<sup>2</sup>. Interpolating these results, a line rate of about 0.75



(a)



(b)

Fig. 12: (a) Measured and simulated scan loss as a function of the scanning angle. (b) Scanning angle as a function of the displacement of the lens from the center feed position.

Hz is achieved for the 50 deg FoV (corresponding to a lens displacement of 2 mm).

With the achieved line rate, the proposed architecture could be used for space sensing applications where the limit is the integration time. For high imaging speeds such as a radar [8], another piezoelectric motor with higher accelerations will be needed.

## V. DISCUSSION AND CONCLUSIONS

Future heterodyne instruments will benefit from using an antenna with integrated beam-scanning capabilities for submillimeter-wave frequencies. The advances in silicon microfabrication together with the miniaturization and reliability of piezo actuator motors have enabled the development of a silicon micro-lens antenna that can perform beam-scanning capabilities.

We have studied the off-axis properties of the silicon micro-lens antenna fed by a leaky-wave feed presented in [1] and we have built a prototype at 550 GHz integrated with a piezo actuator motor. We found excellent agreement between the simulated and measured performances. The proposed antenna has a bandwidth of 15% with 27dB gain at broadside and a gain scanning loss lower than 1dB where achieved for a FoV of 50 degrees.. The used actuator achieves accelerations of



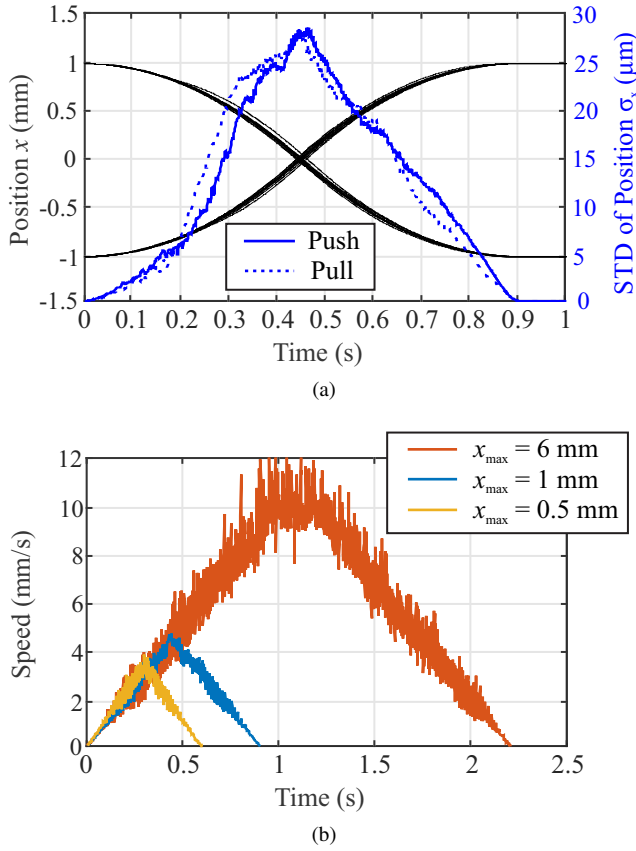


Fig. 13: (a) Position  $x$  as a function of the time for 1 second push and pull continuous movements of 1 mm for 10 push and pull movements (left axis). The standard deviation of the position for each time instant for the 10 push and pull movements. (b) Speed as a function of 2.5 seconds for 0.5 mm, 1 mm and 6 mm continuous displacements of the piezo actuator motor.

$11.5 \text{ mm/s}^2$  with accuracies better than  $28 \mu\text{m}$  for continuous mode operation.

#### ACKNOWLEDGMENT

This work was carried out at the Jet Propulsion Laboratory (JPL), California Institute of Technology, under a contract with the National Aeronautics and Space Administration. Nuria Llombart acknowledges the support by the European Union through the ERC Starting Grant LAA-THz-CC (639749).

#### REFERENCES

- [1] N. Llombart, G. Chattopadhyay, A. Skalare, and I. Mehdi, "Novel terahertz antenna based on a silicon lens fed by a leaky wave enhanced waveguide," *IEEE Transactions on Antennas and Propagation*, vol. 59, no. 6, pp. 2160–2168, June 2011, doi: 10.1109/TAP.2011.2143663.
- [2] A. M. Cook, A. Colaprete, D. Mauro, J. Stupl, A. N. Nguyen, M. A. Kahre, R. M. Haberle, A. Dono Perez, E. A. Uribe, K. D. Bonner, and S. V. Weston, "Aeolus: A mission to observe the thermal and wind environment of mars," in *12th International Academy of Astronautics (IAA) Low-Cost Planetary Mission (LCPM)*, August 2017.
- [3] R. W. Zurek, A. Chicarro, M. A. Allen, J.-L. Bertaux, R. Clancy, F. Daerden, V. Formisano, J. B. Garvin, G. Neukum, and M. D. Smith, "Assessment of a 2016 mission concept: The search for trace gases in the atmosphere of mars," *Planetary and Space Science*, vol. 59, no. 2, pp. 284 – 291, 2011, doi: "https://doi.org/10.1016/j.pss.2010.07.007.

- [4] M. Choukroun, S. Keihm, F. P. Schloerb, S. Gulkis, E. Lellouch, C. Leyrat, P. von Allmen, N. Biver, D. Bockelée-Morvan, J. Crovisier, P. Encrenaz, P. Hartogh, M. Hofstadter, W. H. Ip, C. Jarchow, M. Janssen, S. Lee, L. Rezac, G. Beaudin, B. Gaskell, L. Jorda, H. U. Keller, and H. Sierks, "Dark side of comet 67P/Churyumov-Gerasimenko in Aug.-Oct. 2014. MIRO/Rosetta continuum observations of polar night in the southern regions," *Astronomy and Astrophysics*, vol. 583, p. A28, Nov. 2015, doi: 10.1051/0004-6361/201526181.
- [5] S. Gulkis, M. Frerking, J. Crovisier, G. Beaudin, P. Hartogh, P. Encrenaz, T. Koch, C. Kahn, Y. Salinas, R. Nowicki, R. Irigoyen, M. Janssen, P. Stek, M. Hofstadter, M. Allen, C. Backus, L. Kamp, C. Jarchow, E. Steinmetz, A. Deschamps, J. Krieg, M. Gheudin, D. Bockelée-Morvan, N. Biver, T. Encrenaz, D. Despois, W. Ip, E. Lellouch, I. Mann, D. Muhleman, H. Rauer, P. Schloerb, and T. Spilker, "MIRO: Microwave Instrument for Rosetta Orbiter," *Space Science Reviews*, vol. 128, no. 1, pp. 561–597, Feb 2007, doi: 10.1007/s11214-006-9032-y.
- [6] P. F. Goldsmith, R. Liseau, T. A. Bell, J. H. Black, J.-H. Chen, D. Hollenbach, M. J. Kaufman, D. Li, D. C. Lis, G. Melnick, D. Neufeld, L. Paganí, R. Snell, A. O. Benz, E. Bergin, S. Bruderer, P. Caselli, E. Caux, P. Encrenaz, E. Falgarone, M. Gerin, J. R. Goicoechea, Å. Hjalmarson, B. Larsson, J. Le Bourlot, F. Le Petit, M. De Luca, Z. Nagy, E. Roueff, A. Sandqvist, F. van der Tak, E. F. van Dishoeck, C. Vastel, S. Viti, and U. Yildiz, "Herschel Measurements of Molecular Oxygen in Orion," *Astrophysical Journal*, vol. 737, p. 96, Aug. 2011, doi: 10.1088/0004-637X/737/2/96.
- [7] P. F. Goldsmith, "Sub-millimeter heterodyne focal-plane arrays for high-resolution astronomical spectroscopy," *URSI Radio Science Bulletin*, vol. 2017, no. 362, pp. 53–73, Sept 2017, doi: 10.23919/UR-SIRSB.2017.8267373.
- [8] K. B. Cooper, R. J. Dengler, N. Llombart, B. Thomas, G. Chattopadhyay, and P. H. Siegel, "THz Imaging Radar for Standoff Personnel Screening," *IEEE Transactions on Terahertz Science and Technology*, vol. 1, no. 1, pp. 169–182, Sept 2011, doi: 10.1109/TTHZ.2011.2159556.
- [9] M. Kotiranta, K. Jacob, H. Kim, P. Hartogh, and A. Murk, "Optical Design and Analysis of the Submillimeter Wave Instrument on JUICE," *IEEE Transactions on Terahertz Science and Technology*, pp. 1–1, 2018, doi: 10.1109/TTHZ.2018.2866116.
- [10] G. Physic Instrumente GmbH Co. KG, Karlsruhe, "Physic instrumente." [Online]. Available: <https://www.physikinstrumente.com/>
- [11] C. Jung-Kubiak, T. J. Reck, J. V. Siles, R. Lin, C. Lee, J. Gill, K. Cooper, I. Mehdi, and G. Chattopadhyay, "A multistep drier process for complex terahertz waveguide components," *IEEE Transactions on Terahertz Science and Technology*, vol. PP, no. 99, pp. 1–6, 2016, doi: 10.1109/TTHZ.2016.2593793.
- [12] T. Reck, C. Jung-Kubiak, J. V. Siles, C. Lee, R. Lin, G. Chattopadhyay, I. Mehdi, and K. Cooper, "A silicon micromachined eight-pixel transceiver array for submillimeter-wave radar," *IEEE Transactions on Terahertz Science and Technology*, vol. 5, no. 2, pp. 197–206, March 2015, doi: 10.1109/TTHZ.2015.2397274.
- [13] M. Alonso-delPino, T. Reck, C. Lee, C. Jung-Kubiak, N. Llombart, I. Mehdi, and G. Chattopadhyay, "Micro-lens antenna integrated in a silicon micromachined receiver at 1.9 THz," in *2016 10th European Conference on Antennas and Propagation (EuCAP)*, April 2016, pp. 1–3, doi: 10.1109/EuCAP.2016.7481287.
- [14] M. Alonso-delPino, T. Reck, C. Jung-Kubiak, C. Lee, and G. Chattopadhyay, "Development of Silicon Micromachined Microlens Antennas at 1.9 THz," *IEEE Transactions on Terahertz Science and Technology*, vol. 7, no. 2, pp. 191–198, March 2017, doi: 10.1109/TTHZ.2017.2655340.
- [15] N. Llombart, C. Lee, M. Alonso-delPino, G. Chattopadhyay, C. Jung-Kubiak, L. Jofre, and I. Mehdi, "Silicon Micromachined Lens Antenna for THz Integrated Heterodyne Arrays," *IEEE Transactions on Terahertz Science and Technology*, vol. 3, no. 5, pp. 515–523, Sept 2013, doi: 10.1109/TTHZ.2013.2270300.
- [16] M. Alonso-delPino, N. Llombart, G. Chattopadhyay, C. Lee, C. Jung-Kubiak, L. Jofre, and I. Mehdi, "Design Guidelines for a Terahertz Silicon Micro-Lens Antenna," *IEEE Antennas and Wireless Propagation Letters*, vol. 12, pp. 84–87, 2013, doi: 10.1109/LAWP.2013.2240252.
- [17] M. J. M. van der Vorst, P. J. I. de Maagt, and M. H. A. J. Herben, "Scan-Optimized Integrated Lens Antennas," in *1997 27th European Microwave Conference*, vol. 1, Sept 1997, pp. 605–610, doi: 10.1109/EUMA.1997.337751.
- [18] D. F. Filipovic, G. P. Gauthier, S. Raman, and G. M. Rebeiz, "Off-axis properties of silicon and quartz dielectric lens antennas," *IEEE Transactions on Antennas and Propagation*, vol. 45, no. 5, pp. 760–766, May 1997, doi: 10.1109/8.575618.



- [19] J. R. Costa, M. G. Silveirinha, and C. A. Fernandes, "Evaluation of a Double-Shell Integrated Scanning Lens Antenna," *IEEE Antennas and Wireless Propagation Letters*, vol. 7, pp. 781–784, 2008, doi: 10.1109/LAWP.2008.2008403.
- [20] P. F. Goldsmith, *Quasioptical Systems: Gaussian Beam Quasioptical Propagation and Applications*. IEEE Press, 1998.
- [21] A. Neto, S. Maci, and P. J. I. D. Maagt, "Reflections inside an elliptical dielectric lens antenna," *IEE Proceedings - Microwaves, Antennas and Propagation*, vol. 145, no. 3, pp. 243–247, June 1998, doi: 10.1049/ip-map:19981884.
- [22] "CST Microwave Studio." [Online]. Available: <http://cst.com>
- [23] L. E. Busse, C. M. Florea, J. A. Frantz, L. B. Shaw, I. D. Aggarwal, M. K. Poutous, R. Joshi, and J. S. Sanghera, "Anti-reflective surface structures for spinel ceramics and fused silica windows, lenses and optical fibers," *Opt. Mater. Express*, vol. 4, no. 12, pp. 2504–2515, Dec 2014, doi: 10.1364/OME.4.002504.
- [24] T. Nitta, S. Sekiguchi, Y. Sekimoto, K. Mitsui, N. Okada, K. Karatsu, M. Naruse, M. Sekine, H. Matsuo, T. Noguchi, M. Seta, and N. Nakai, "Anti-reflection Coating for Cryogenic Silicon and Alumina Lenses in Millimeter-Wave Bands," *Journal of Low Temperature Physics*, vol. 176, no. 5, pp. 677–683, Sep 2014, doi: 10.1007/s10909-013-1059-3.
- [25] S. J. C. Yates, A. M. Baryshev, O. Yurduseven, J. Bueno, K. K. Davis, L. Ferrari, W. Jellema, N. Llombart, V. Murugesan, D. J. Thoen, and J. J. A. Baselmans, "Surface Wave Control for Large Arrays of Microwave Kinetic Inductance Detectors," *IEEE Transactions on Terahertz Science and Technology*, vol. 7, no. 6, pp. 789–799, Nov 2017, doi: 10.1109/TTHZ.2017.2755500.



**Maria Alonso del Pino** (S'10-M'14) received her degree in Telecommunications Engineering from the Technical University of Catalonia (Barcelona, Spain) in 2008; her M.S. in Electrical Engineering from the Illinois Institute of Technology, Chicago, IL, USA in 2008; and her Ph.D. degree in Signal Theory and Communications/Electrical Engineering from the Technical University of Catalonia, Barcelona, Spain in 2013.

From 2014 to 2015 she was as a postdoctoral researcher at the Technical University of Delft, Delft, Netherlands. From 2015 to 2016, she was a NASA postdoctoral fellow at the Jet Propulsion Laboratory, Pasadena (JPL), CA, USA. Currently, she is a member of the technical staff at the Sub-millimeter Wave Advanced Technology group of JPL. Her interests include millimeter and submillimeter-wave heterodyne and direct detection receiver technologies, antennas, quasioptical systems.

She is the co-recipient of the 2014 IEEE Terahertz Science and Technology Best Paper Award and the recipient of the Outstanding Reviewer Award by IEEE Terahertz Science and Technology Transactions in 2013.



**Cecile Jung-Kubiak** (M'15, SM'16) received her master's degree in Physics and Materials Chemistry from Polytech'Montpellier, France in 2006 and her PhD degree in Physics from Universite Paris-Sud XI, France in 2009. She was the recipient of a 2-year NASA Postdoctoral Fellowship at the California Institute of Technology in 2010, and she is now a member of the Technical Staff for the S.W.A.T. group of the Jet Propulsion Laboratory, in Pasadena, USA. Her research interests include the development of silicon micromachining technologies using DRIE

techniques, the miniaturization of multi-pixel arrays to build compact 3-D instruments and GaAs-based frequency multipliers and mixers in the THz region. She has co-authored over 60 papers in international journals and conferences, holds several patents and was a recipient of the 2010 JPL Outstanding Postdoctoral Research Award in the field Technology, Instrumentation, and Engineering and the 2014 IEEE THz Science and Technology Best Paper Award.



**Theodore Reck** (M'04-SM'15) received the B.S. degree in electrical engineering from the University of Texas at Austin in 2000 and PhD in Electrical Engineering at the University of Virginia in 2010.

From 2010 to 2013 he was a NASA postdoctoral fellow at the Jet Propulsion Laboratory (JPL) designing terahertz devices that utilize silicon micro-machining packaging. Presently he is a member of the technical staff at JPL. Currently, his research interests include RF-MEMS, terahertz metrology, and cryogenic MMIC LNAs.



**Nuria Llombart** (S'06-M'07-SM'13) received the master's degree in electrical engineering and the Ph.D. degree from the Polytechnic University of Valencia, Valencia, Spain, in 2002 and 2006, respectively.

During her Master's degree studies, she spent one year at the Friedrich-Alexander University of Erlangen-Nuremberg, Erlangen, Germany, and was with the Fraunhofer Institute for Integrated Circuits, Erlangen. From 2002 to 2007, she was with the Antenna Group, TNO Defense, Security and Safety

Institute, The Hague, The Netherlands, as a Ph.D. student and then a Researcher. From 2007 to 2010, she was a Post-Doctoral Fellow with the California Institute of Technology, Pasadena, CA, USA, where she was with the Submillimeter Wave Advance Technology Group, Jet Propulsion Laboratory. She was a "Ramón y Cajal" Fellow with the Optics Department, Complutense University of Madrid, Madrid, Spain, from 2010 to 2012. In 2012, she joined the THz Sensing Group, Technical University of Delft, Delft, The Netherlands, where she is currently a Full Professor. She has co-authored over 150 journal and international conference contributions. Her current research interests include the analysis and design of planar antennas, periodic structures, reflector antennas, lens antennas, and waveguide structures, with emphasis in the terahertz range.

Dr. Llombart was the recipient H. A. Wheeler Award for the Best Applications Paper of 2008 in the IEEE TRANSACTIONS ON ANTENNAS AND PROPAGATION, the 2014 THz Science and Technology Best Paper Award of the IEEE Microwave Theory and Techniques Society, several NASA awards, and the 2014 IEEE Antenna and Propagation Society Lot Shafai Mid-Career Distinguished Achievement Award. In 2015, she was the recipient of European Research Council Starting Grant. She serves as a Board Member of the IRMMW-THz International Society..



**Goutam Chattopadhyay** (S'93-M'99-SM'01-F'11) is a Senior Research Scientist at the NASA's Jet Propulsion Laboratory, California Institute of Technology, and a Visiting Associate at the Division of Physics, Mathematics, and Astronomy at the California Institute of Technology, Pasadena, USA. He received the B.E. degree in electronics and telecommunication engineering from the Bengal Engineering College, Calcutta University, Calcutta, India, in 1987, the M.S. degree in electrical engineering from the University of Virginia, Charlottesville, in 1994,

and the Ph.D. degree in electrical engineering from the California Institute of Technology (Caltech), Pasadena, in 1999. From 1987 until 1992, he was a Design Engineer with the Tata Institute of Fundamental Research (TIFR), Pune, India.

His research interests include microwave, millimeter-, and submillimeter-wave heterodyne and direct detector receivers, frequency sources and mixers in the terahertz region, antennas, SIS mixer technology, direct detector bolometer instruments; InP HEMT amplifiers, mixers, and multipliers; high frequency radars, and applications of nanotechnology at terahertz frequencies. He has more than 300 publications in international journals and conferences and holds more than fifteen patents. Among various awards and honors, he was the recipient of the Best Undergraduate Student Award from the University of Calcutta in 1987, the Jawaharlal Nehru Fellowship Award from the Government of India in 1992, and the IEEE MTT-S Graduate Fellowship Award in 1997. He was the recipient of the best journal paper award in 2013 by IEEE Transactions on Terahertz Science and Technology, and IETE Prof. S. N. Mitra Memorial Award in 2014. He also received more than 30 NASA technical achievement and new technology invention awards. He is an associate editor of the IEEE Transactions on Antennas and Propagation, a Fellow of IEEE (USA) and IETE (India) and an IEEE Distinguished Lecturer.